John von Neumann Institute for Computing

Numerical Investigations of Complex Nano-Systems

M. Dreher, D. Fischer, K. Franzrahe, G. Günther,
P. Henseler, J. Hoffmann, W. Strepp, P. Nielaba

published in

NIC Symposium 2004, Proceedings,
Dietrich Wolf, Gernot Münster, Manfred Kremer (Editors),
John von Neumann Institute for Computing, Jülich,
NIC Series, Vol. **20**, ISBN 3-00-012372-5, pp. 291-300, 2003.

http://www.fz-juelich.de/nic-series/volume20

Numerical Investigations of Complex Nano-Systems

M. Dreher, D. Fischer, K. Franzrahe, G. Günther, P. Henseler, J. Hoffmann, W. Strepp, and P. Nielaba

Physics Department (Theory), University of Konstanz, 78457 Konstanz, Germany
E-mail: markus.dreher@uni-konstanz.de, fis@zurich.ibm.com
{*kerstin.franzrahe, guido.guenther, peter.henseler*}*@uni-konstanz.de*
jhoffmann@itwm.fraunhofer.de, peter.nielaba@uni-konstanz.de

Quantum effects, structures and phase transitions in Nano-systems have been studied. An overview is given on the results of our computations on atomic wires, clusters, pore condensates, Bose fluids, elastic properties of model colloids and model colloids in external fields.

1 Introduction and General Remarks

Nanostructures in reduced geometry have become an interesting research domain in the last years. Despite the fact that by experimental techniques many structural-, elastic-, electronic- and phase- properties of systems in the size of a few nanometers have been obtained, the theoretical investigations and analyses are still in an initial stage. This is partly due to the fact that systems which are far away from the thermodynamic limit (with infinitely many particles) due to their finite size are difficult to handle by analytical methods which are suitable for systems with either few particles (2-5) or in the limit of infinitely many particles. In this field computer simulations have become more and more important since nano-systems in reduced geometry contain about 10-10.000 particles, which is nearly ideal for the application of computer simulation methods. Many important results have been obtained by the support of HPC centers (NIC, HLRS, SSC)[1,2].

Our research on nanostructures is embedded in the Sonderforschungsbereich 513 with two projects (A11 and B10), in the Transregio-SFB TR6 with project C4, and with a project in a European Graduate College on soft matter. Besides this our activities are linked to recent research goals in the European-Science-Foundation programme "Challenges in Molecular Simulations: Bridging the Length- and Time- Scale Gap (SIMU)" (http://simu.ubl.ac.be).

The present work contains several new insights into pore condensates and phase transitions and quantum effects in nano-systems in external potentials and reduced geometry. In the path integral formulation of the partition function a quantum particle is represented by a classical chain of P "Trotter particles" (P$\rightarrow \infty$), where each Trotter particle interacts harmonically with its neighbors on the chain and interactions between the quantum particles are always at the same Trotter particle index. In the path integral simulations performed on the T3E a very efficient parallel algorithm along the chain-coordinate could be utilized, putting the system at a given Trotter particle index on one processor, which allowed us to approach the quantum limit properly by using 64 processors in parallel (P=128), the algorithm only scaling with P. This good scaling property with P allowed us to compute full phase diagrams of the systems, which otherwise had been a hopeless task. In addition the Monte Carlo procedure employed requires the computation of statistical averages which can be done very efficiently if averages of system replicas with different initial conditions are computed in parallel on several processors.

2 Electronic and Structural Properties of Nano Wires

In this part of the project the structural and electronic properties of atomic gold wires have been computed. Such systems were studied recently by experimental methods[4–6], where wires have been stretched down to single atom contacts. In this context nanocontacts under stress have been simulated[7] using three different interactions: the 'surface embedded atom'-interaction with a (up to 70 %) reduced electron density turned out to be not sufficiently stable, with Lennard-Jones interactions shifts of planes and single-atom contacts have been observed, however no atom chains. In case of the stretching of a nanocontact with interactions according to the 'effective medium theory' (EMT)[8] single atom contacts as well as atom chains have been found (top of fig. 1). In order to prevent the heating of the wire due to the stretching work, a Nosé-Hoover thermostat has been implemented in the molecular dynamics simulation.

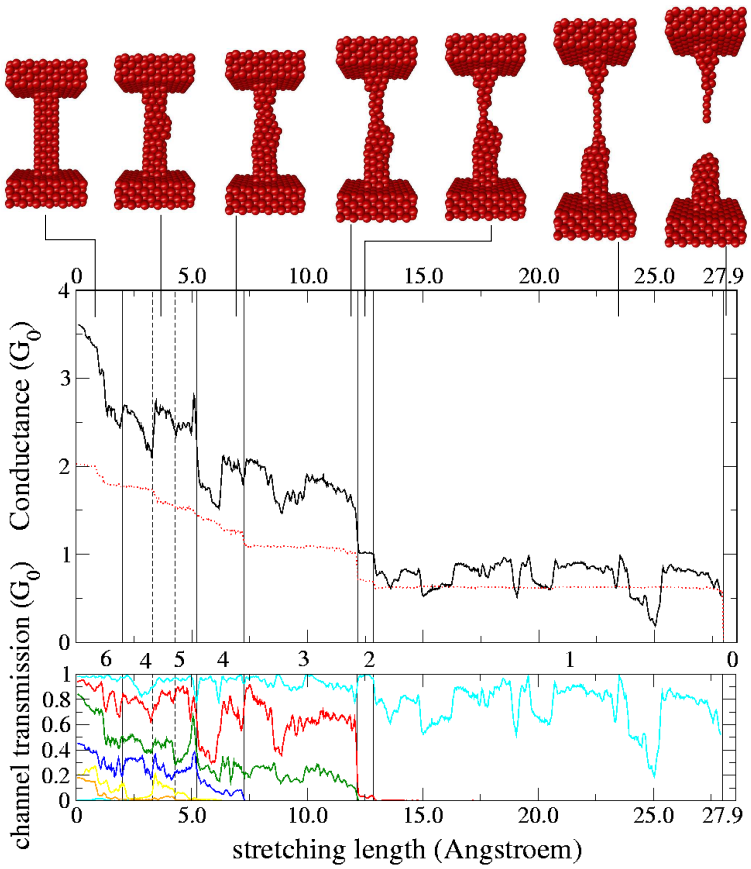

Figure 1. **Upper panel**: total transmission (black) in units of $G_0 = 2e^2/h$ & minimal effective radius (red dashed) in arbitrary units as a function of the stretching length (T=4.2K). **Lower panel**: shows the single channels; perpendicular lines: define regions with different channel numbers (written between the panels).

In cooperation with JAN HEURICH and CARLOS CUEVAS, who developed[9] -by using a tight-binding-model and Green function techniques- a program for the current through a nanocontact, conductivity curves (in different channels) have been determined[7]. In figure 1 in the top panel the total transmission (black) in units of $G_0 = 2e^2/h$ and the radius of the minimum cross section[10] perpendicular to the stretching direction (red dashed) in arbitrary units as a function of the stretching length are shown (T=4.2K). The lower panel shows the contribution of the individual channels. The vertical black lines define regions with different channel numbers.

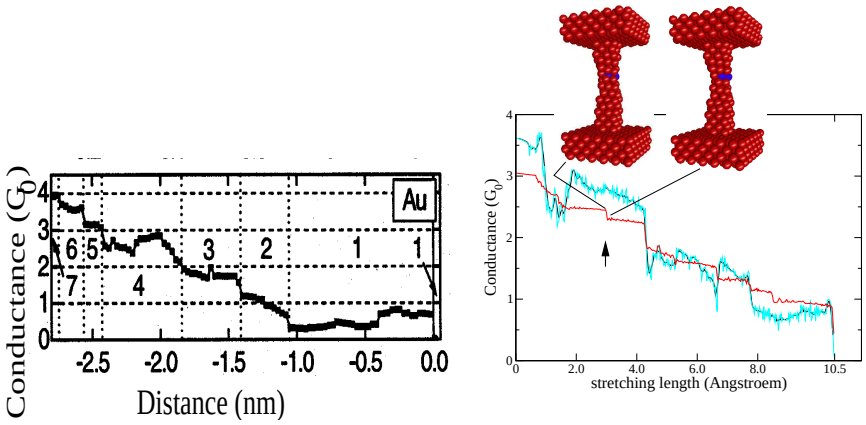

Figure 2. **Left**: Conductance measurement of Gold as function of distance (zero corresponds to the break of the nano wire)($T < 100$mK); numbers in the figure: experimentally measured channel numbers. From Ref. 5. **Right**: Total conductance (blue), averaged over 5 adjacent configurations (black) and radius of the minimum cross section (red) in function of the stretching length[7].

We would like to emphasize the following results:

- *change of effective radius- & conductance*: if there are only few atoms at the contact point, an abrupt atom rearrangement (jump of the red effective radius curve) is correlated with the breakdown of individual channels.
- *effective radius constant & change of conductance*: The conductance is not totally determined by the atoms of the constriction: e.g. in Fig. 1 between the first, vertical black line and the first dashed line: the effective radius (red dashed) changes hardly, but the conductance falls off. Reason: atom rearrangements in the vicinity of the constriction.
- *jump of the effective radius & no jump of the conductance* for example in Fig. 2 (right side): the upper both atoms migrate from the narrowest constriction. That's why the partly covered, blue atoms become uncovered (minimal effective radius (red) jumps). The conductance, however, does not jump at this point, but decreases gradually due to atom rearrangements in the vicinity of the constriction.

The conductance through an atom wire is slightly smaller than G_0 and only one channel contributes (Fig. 1). The qualitative agreement with the experiment (Fig. 2 (left side): $T < 100$mK; the numbers in the plot denote the number of channels) is good, the conductivity fluctuations seem to be slightly higher compared to the experiment.

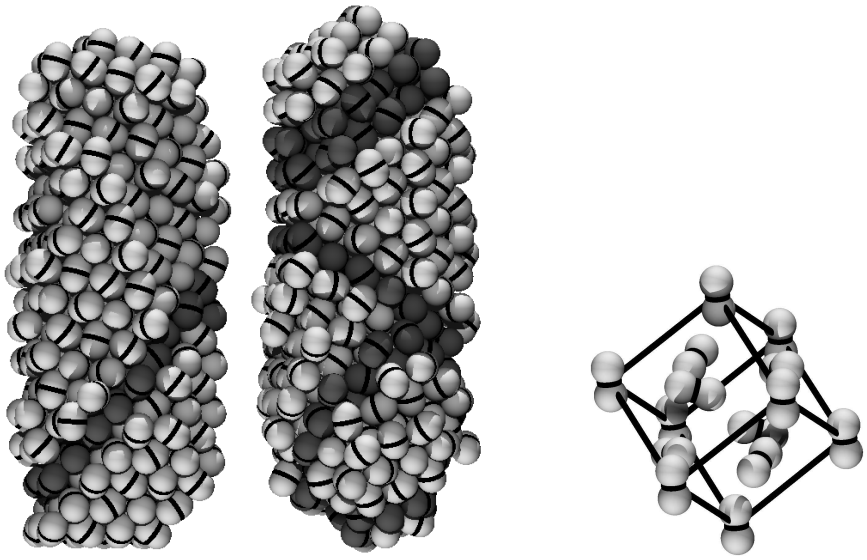

Figure 3. Solid CO- (left) and N_2- pore condensate in a hard $R = 14$ Å-pore at 2 K. Light: Particles with FCC-type neighborhood. Dark: HCP-type neighborhood. Particles, which cannot assigned be to any symmetry, are not shown (border particles). Top: a FCC- cell taken from the CO- pore condensate.

Because every stretching process is a little bit different, at the moment we are calculating conductance histograms[7] which were directly measured in experiments. In future work we plan to apply Car-Parrinello methods for the computation of the atomic configurations near the constriction[7]. Such methods have been used recently for the computation of structural and electronic properties of Si_4-clusters on solid surfaces[3].

3 Phase Transitions in Nano-Pores

Another research topic in our NIC-project were structures, phase transitions and quantum effects in pore condensates, which we studied by a combination of finite-size-scaling methods and PIMC [11–14]. The effect of the finite pore diameter and the strength of the interaction between the particle and the cylinder wall on the structures and phase diagrams has been computed, in particular in the solid phase. Besides a reduction of the critical temperature of the adsorbate-condensate phase transition with decreasing pore diameter several interesting effects on the crystallization scenario have been found. In case of strong particle-wall interactions the system freezes at low temperatures in layers from the cylinder wall to the axis, in case of weak particle-wall interactions solid structures appear locally, which are known from bulk-materials. The crystallization process can consist of two stages, in which parts of the system close to the cylinder wall freeze at a higher temperature than the rest of the system at the pore axis. In experiments[15] two stages crystallization phenomena have been observed as well. Besides this solid-liquid- interfaces with meniscus shape have been found in our studies. Quantum effects on phase diagrams have been quantified by the path integral Monte Carlo method, which is briefly described below:

Canonical averages $< A >$ of an observable A in a system defined by the Hamiltonian

$\mathcal{H} = E_{kin} + V_{pot}$ of N particles in a volume V are given by:

$$\langle A \rangle = Z^{-1} \quad \mathrm{tr} \quad [A \exp(-\beta \mathcal{H})] \quad . \tag{1}$$

Here $Z = \mathrm{tr} \quad [\exp(-\beta \mathcal{H})]$ is the partition function and $\beta = 1/k_B T$ is the inverse temperature. Utilizing the Trotter–product formula,

$$\exp(\beta \mathcal{H}) = \lim_{P \to \infty} \left(\exp(-\beta E_{kin}/P) \exp(-\beta V_{pot}/P)\right)^P \quad , \tag{2}$$

we obtain the path integral expression for the partition function:

$$Z(N,V,T) = \lim_{P \to \infty} \left(\frac{mP}{2\pi\beta\hbar^2}\right)^{3NP/2} \prod_{s=1}^{P} \int d\{\mathbf{r}^{(s)}\} \cdot \tag{3}$$

$$\cdot \ \exp\left\{-\frac{\beta}{P}\left[\sum_{k=1}^{N} \frac{mP^2}{2\hbar^2\beta^2}(\mathbf{r}_k^{(s)} - \mathbf{r}_k^{(s+1)})^2 + V_{pot}(\{\mathbf{r}^{(s)}\})\right]\right\}$$

Here, m is the particle mass, integer P is the Trotter number and $\mathbf{r}_k^{(s)}$ denotes the coordinate of particle k at Trotter-index s, and periodic boundary conditions apply, $P + 1 = 1$. This formulation of the partition function allows us to perform Monte Carlo simulations[16] for increasing values of P approaching the true quantum limit for $P \to \infty$. Thermal averages in the ensemble with constant pressure p are given via the corresponding partition function $\Delta(N,p,T) = \int_0^\infty dV \exp[-\beta p V] Z(N,V,T)$.

For light (Ne) particles the critical temperature and the condensate density is reduced by about 10 % compared to the classical case. The quantum mechanical ground state oscillations destabilize the system and result in smaller phase transition temperatures. Structural changes due to ground state oscillations have been found as well, in particular the occupancy of positions on the cylinder axis due to packing effects have been analyzed for light and heavy particles. As an important conclusion of our studies it turns out, that a complete overview on the fluid and solid structures and phase diagrams in pore condensates at low temperatures can only be obtained by taking the quantum effects into account- which can be done efficiently by PIMC. Based on these results, we investigate[11,17] the properties of molecular pore condensates (N_2, CO). Our studies[11,17] show that at low temperatures interesting solid structures appear, in which particles locally have FCC- or HCP- neighborhood, s. Fig. 3. The influence of the quantum mechanics and the strength of the particle-wall interaction and the pore diameter as well as the new phase transitions due to the molecular orientational degrees of freedom will be analyzed.

4 PIMC - Studies of Hard Bose Fluids

Exploiting path integral Monte Carlo methods we studied[18] the behavior of the fluid phase of quantum mechanical hard sphere- and disk- systems including the superfluid phase transition. The partition function for a bosonic system is obtained by - in addition to Eq. (3) - taking into account the connectivity of the permutations $\mathcal{P}$ of the Trotter-chain end points of Bose particles with the Trotter-chain starting points of other Bose particles. By sampling the winding number $\mathbf{W}$ we analyzed the superfluid fraction[19]:

$$\frac{\rho_S}{\rho} = \frac{m}{\hbar^2} \frac{\langle \mathbf{W}^2 \rangle L^2}{2\beta N} + \mathcal{O}(\mathbf{v}^4) \ , \tag{4}$$

where L is the side length of the simulation box, ρ is the density, ρ_S is the superfluid density, and the winding number is the number of times we have to invoke periodic boundary

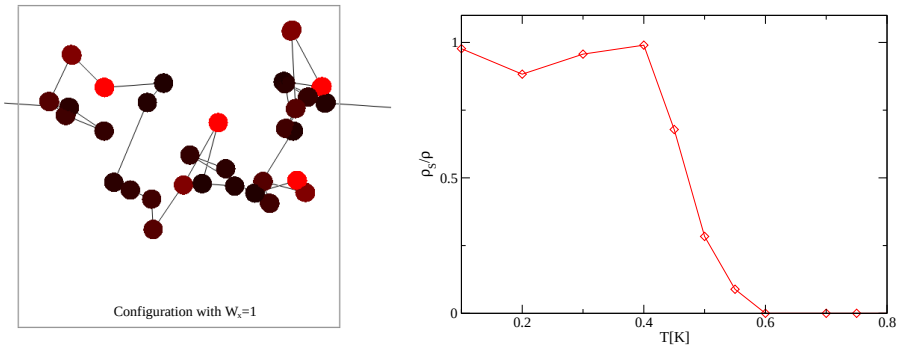

Figure 4. **Left side:** Connected Trotter chains for two dimensional hard Bose fluids (P=8) in a configuration with $W_x = 1$. **Right side:** Superfluid fraction of a two dimensional hard Bose fluid with particles of diameter $\sigma = 2.56$ Å and mass $m = 4u$ at a density $\rho^* = 0.282$ (N=23, P=8).

conditions when following a path: $\sum_{i=1}^{N}(\mathbf{r}_{\mathcal{P}_i} - \mathbf{r}_i) = \mathbf{W}L$. In Fig. 4 we show a typical connected Trotter chain spreading over the box and the superfluid fraction of a two dimensional hard Bose fluid as a function of temperature for P=8. The transition is rounded due to the finite size of the system (N=23). Further studies of the effect of external potentials on the Bose condensation are scheduled.

5 Elastic and Structural Properties of Model Colloids

Other research topics which have been studied by us aim at a better understanding of the properties of colloidal systems in two dimensions. Since about 40 years the nature of the melting transition in the system of hard disks with translational degrees of freedom in

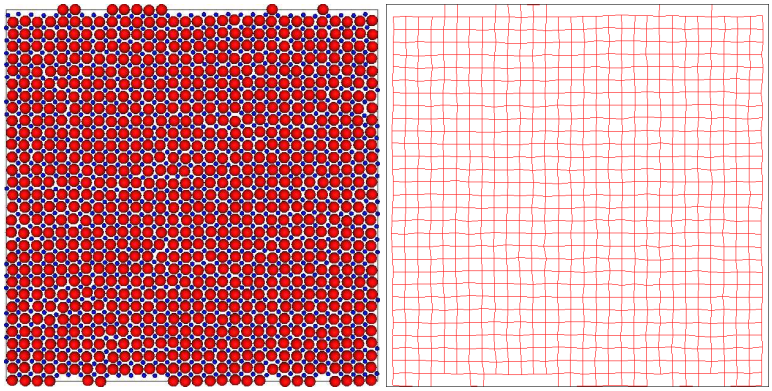

Figure 5. NpT-Simulation of a binary mixture (particle fraction $p = 0.5$) of $N = 1800$ hard discs with a diameter ratio of $a = 0.414$ at a pressure of $p^* = 36$. This is a snapshot of the configuration after 11000000 Monte Carlo steps. The right hand picture shows connection lines between particles of the same species, which are next neighbours (distance $\leq 1.4\cdot$ particle diameter)[20].

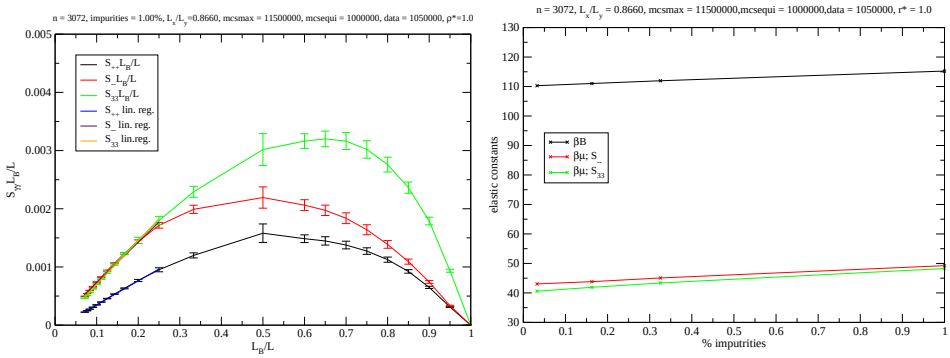

Figure 6. **Left**: NVT-Simulation of the quenched strain-strain fluctuations (for definitions see Ref. 22) versus relative subsystem length L_b/L of a hard disk system ($N = 3072$) with 1% (immobile) point-impurities[20]. For 100 arbitrary placements of the impurities in the initial configuration simulations were performed, that evaluated 550000 data points each. **Right**: Elastic constants versus impurity concentration obtained from the NVT-Simulations of a hard disk system with $N = 3072$ particles and a varying percentage of point-impurities.With the slopes S_{++}, S_{--} and S_{33} of the linear regression functions of the linear part of the strain-strain fluctuation curves the elastic constants $\beta B = \frac{1}{2S_{++}}$, $\beta\mu = \frac{1}{2S_{--}} - P^*$ and $\beta\mu = \frac{1}{2S_{33}} - P^*$ were calculated. The pressure was calculated from the free volume expression $P^* = 2\rho/(2\sqrt{3}\rho - 1)$[20].

two dimensions is under debate in the literature. By a new finite-size-scaling procedure[22] the elastic constants in this system have been analyzed[24,25]. According to these results the behavior of the system is consistent with the predictions of the KTHNY theory[23,26]. By application of such a method to configurations obtained experimentally by video mi-

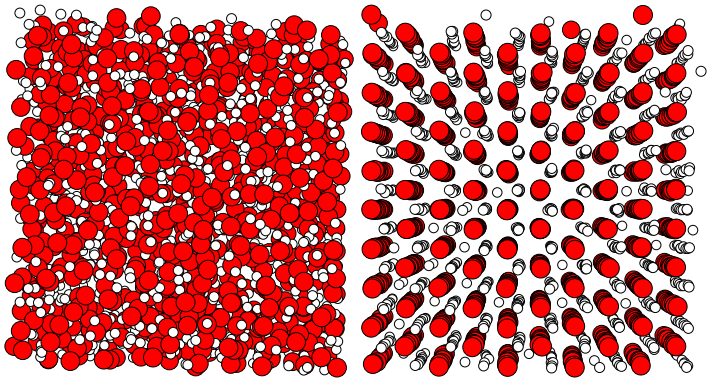

Figure 7. Configurations from a NpT-Simulation of a A-B hard sphere mixture (3D) with $N = 1620$ particles, diameter ratio 0.5272 and concentration $x_A = 0.5$. **Left side**: Disordered configuration at $p = 40$, starting configuration: perfect AB_2 ordered structure; **Right side**: Slightly disordered configuration at $p = 70$, starting configuration: perfect AB_2 ordered structure[21]. The AB_2 packing arrangement consists of layers of large closed-packed A particles, which are aligned directly above each other along the c axis normal to the layer. The B particles fill all the hexagonal cavities forming intervening layers. The size ratio was chosen in such a way, that the small B particles exactly fit into the cavities when each large particle is in contact with its neighbors. All the particles are shown with half of their diameter for clarity reasons.

croscopy methods it was possible to analyze precisely experimental results on the elasticity of colloidal systems[36].

In future studies we plan to analyze in detail colloidal mixtures with different diameters in two[20] and three[21] dimensions, and to study the composition dependency of their phase behavior and the elastic properties. A priori it is not obvious if such systems are softer or harder compared to the corresponding monodisperse systems, and a systematic study is required in order to design materials with well defined elastic properties at a later stage. Besides this, already in two spatial dimensions interesting structures have been found which significantly deviate from the traditional triangular lattice for certain diameter ratios, s. Fig. 5. In Fig. 6 elastic constants for hard disk systems with additional immobile point impurities have been computed. Already for a concentration of 1 % impurities a strong increase of the shear modulus by about 25% is found compared to the pure hard disk system. In case of hard sphere mixtures in 3D interesting solid structures at high pressures have been found as well, see Fig. 7.

The nature of the phase transitions in systems with elliptical particle shapes is of great interest as well, since in this case soft and hard "directions" exist in the solid (parallel and perpendicular to the main particle axes) and deviations from the KTHNY scenario can be expected. Such systems shall be studied in the future as well as systems with antiferromagnetic interactions.

6 Quantum Effects on Phase Diagrams of Nano-Systems in External Potentials

Hard and soft disks in external periodic potentials show rich phase diagrams with freezing and melting phase transitions when the density of the system is varied[27]. In the NIC-project large scale Monte Carlo simulations have been done in order to determine the phase diagram by detailed finite-size-scaling analyses of different thermodynamic quantities like the order parameter, its cumulants and other quantities for various values of the density and amplitude of the external potential[28–30, 32–34]. In case of hard disks we found clear evidence for the appearance of a reentrant fluid phase over a significant region of parameter values[29]. We thus have shown by our simulations, that the hard disk system has a phase behavior as it is known from experiments with charge stabilized colloids[27], a system which undergoes a phase transition from a fluid to a solid phase with increasing amplitude of a periodic laser field, and for larger amplitudes another phase transition to a reentrant fluid phase. Our data are in partial agreement with the results of a theory of laser induced melting.

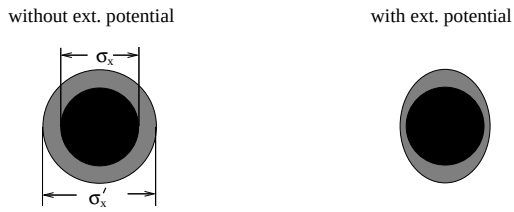

Figure 8. Schematic picture of the effect of an external periodic potential of the form $V(x, y) = V_0 \sin(x/a)$ on the "effective" diameter of quantum hard disks.

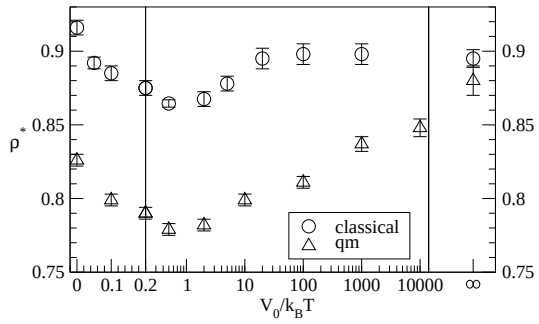

Figure 9. Phase diagram in the density ($\rho^* = \rho\sigma^2$)- potential amplitude (V_0/k_BT)- plane for a system with N=400 particles, $m^* = mT\sigma^2 = 10.000$ ("qm") and $m^* = \infty$ (classical) and Trotter order $P = 64$.

The differences and similarities of the systems with weak potentials (DLVO, $1/r^{12}$) and the relation to the experiment have been analyzed[30, 33, 34].

These results shall be completed by further comparative studies. Besides these classical studies we explore the validity of our results on atomic length scales. In this context we were able to investigate the properties of quantum hard disks with a finite particle mass m and interaction diameter σ in an external periodic potential by PIMC[28, 35]. Due to the quantum delocalization effect a larger effective particle diameter results, and in the external potential this delocalization is asymmetrical: in the direction perpendicular to the potential valleys we obtain a stronger particle localization than parallel to the valleys, s. Fig. 8. As a result the reentrance region in the phase diagram is significantly modified in comparison to the classical case, s. Fig. 9. Due to the larger quantum "diameter" the transition densities at small potential amplitudes are reduced in comparison to the classical values. At large amplitudes the classical and quantum transition densities merge. This effect is due to the approach of the effective quantum disk size to the classical value in the direction perpendicular to the potential valleys and leads to the surprizing prediction, that the quantum crystal in a certain density region has a direct transition to the phase of the modulated liquid by an increase of the potential amplitude. This scenario is not known in the classical case. We plan to explore this interesting topic for systems with different particle masses by PIMC studies and finite-size-scaling methods. Besides this we plan to analyze the order of the phase transition at high potential amplitudes by an application of our new method for the computation of elastic constants. The influence of a potential with higher symmetry shall be explored as well as the effect of the potential amplitude on the Bose condensation in case of systems with Bose statistics.

Acknowledgements

We grateful acknowledge useful discussions with W. Andreoni, C. Bechinger, K. Binder, C. Cuevas, J. Heurich, E. Scheer and S. Sengupta, support by the SFB 513, the SFB-TR6, the European Graduate College on Soft Matter and the DFG (Ni 259/8-2), and granting of computer time from the NIC.

References

1. P. Nielaba, in: *Computational Methods in Surface and Colloid Science*, M. Borowko (Ed.), Marcel Dekker Inc., New York (2000), pp.77-134.
2. *Bridging Time Scales: Molecular Simulations for the Next Decade*, edited by P. Nielaba, M. Mareschal, G. Ciccotti, Springer, Berlin (2002).
3. M.Grass,D.Fischer,M.Mathes,G.Ganteför, P.Nielaba, Appl.Phys.Lett.**81**,3810 (2002).
4. E. Scheer, P. Joyez, D. Esteve, C. Urbina, M. Devoret, PRL, **78**, 3535 (1997).
5. E. Scheer, N. Agra"it, J. Cuevas, A. Yeyati, B. Ludoph, A. Rodero, G. Bollinger, J. Ruitenbeek, C. Urbina, Nature, **394**, 154 (1998).
6. E.Scheer, W.Belzig, Y.Naveh, M.Devoret, D.Esteve, C.Urbina, PRL, **86**, 284 (2000).
7. Markus Dreher, Diplomarbeit, Konstanz (2002); Ph.D. thesis (in work).
8. K.W. Jacobsen, P. Stoltze, J.K. Nørskov, Surf. Sci., **366**, 394 (1996).
9. J.C. Cuevas, A. Yeyati, A. Martin-Rodero, PRL, **80**, 1066 (1998).
10. Bratovsky, A. Sutton, T. Todorov, PRB, **52**, 5036 (1995).
11. J. Hoffmann, Ph.D.-thesis, University of Konstanz (2002).
12. J. Hoffmann, P. Nielaba, Phys. Rev **E67**, 036115 (2003).
13. J. Hoffmann, P. Nielaba, in *High Performance Computing in Science and Engineering 01*, edited by E. Krause and W. Jäger, Springer, Berlin (2002) pp.92.
14. J. Hoffmann, P. Nielaba, in *Computer Simulation Studies in Condensed Matter Physics XV*, ed. by D.P. Landau, S.P. Lewis, H.-B. Schüttler, Springer, Berlin (2003).
15. D. Wallacher, K. Knorr, Phys. Rev. **B63**, 104202 (2001).
16. D.P. Landau and K. Binder, *A Guide to Monte Carlo Simulations in Statistical Physics*, Cambridge University Press (2000).
17. J. Hoffmann, P. Nielaba (in preparation).
18. G. Günther, Ph.D. thesis (in work).
19. E.L. Pollock, D.M. Ceperley; Phys. Rev. **B 36**, 8343 (1987).
20. K. Franzrahe, Ph.D. thesis (in work).
21. P. Henseler, Ph.D. thesis (in work).
22. S. Sengupta, P. Nielaba, M. Rao, K. Binder, Phys. Rev. **E 61**, 1072 (2000).
23. J. M. Kosterlitz, D. J. Thouless, J. Phys. **C 6**, 1181 (1973); B.I.Halperin and D.R.Nelson, PRL **41**,121(1978); D.R.Nelson and B.I.Halperin, PR **B19**, 2457 (1979); A.P. Young, PR **B 19**, 1855 (1979).
24. S.Sengupta,P.Nielaba,K.Binder, PR**E61**,6294 (2000).
25. K. Binder, S. Sengupta, P. Nielaba, J. Phys.: Cond. Mat. **14**, 2323 (2002).
26. E.Frey,D.R.Nelson,L.Radzihovsky,PRL**83**,2977(1999).
27. C. Bechinger, M. Brunner, P. Leiderer, Phys. Rev. Lett. **86**, 930 (2001).
28. W. Strepp, Ph.D-thesis, Univ. of Konstanz (2003).
29. W. Strepp, S. Sengupta, P. Nielaba, Phys. Rev. **E63**, 046106 (2001).
30. W. Strepp, S. Sengupta, P. Nielaba, Phys. Rev. **E66**, 056109 (2002).
31. K. Binder, Z. Phys. **B43**, 119 (1981); K. Binder, Phys. Rev. Lett. **47**, 693 (1981).
32. M. Lohrer, Diplom-thesis, Univ. of Konstanz (2001).
33. W.Strepp,S.Sengupta,M.Lohrer, P.Nielaba, Math. and Comp. in Simul.**62**, 519 (2003).
34. W.Strepp, S.Sengupta, M.Lohrer, P.Nielaba, Comp. Phys. Commun. **147**, 370 (2002).
35. W. Strepp, P. Nielaba, in preparation.
36. K.Zahn, A.Wille, G.Maret, S.Sengupta, P.Nielaba; Phys.Rev.Lett. **90**, 155506 (2003).